

Ricard V. Solé^{1,2,3}, Bartolo Luque³ and Stuart Kauffman²

¹*Complex Systems Research Group, Department of Physics - FEN
Universitat Politècnica de Catalunya, Campus Nord B5, 08034 Barcelona (Spain).*

²*Santa Fe Institute, 1399 Hyde Park Road, Santa Fe, New Mexico (USA),*

³*Centro de Astrobiología (CAB-NASA), Ciencias del Espacio, INTA,
Carretera de Ajalvir km. 4, 28850 Torrejón de Ardoz, Madrid (Spain).*

The critical boundaries separating ordered from chaotic behavior in randomly wired S -state networks are calculated. These networks are a natural generalization of random Boolean nets and are proposed as an extended approach to genetic regulatory systems, sets of cells in different states or collectives of agents engaged into a set of S possible tasks. An order parameter for the transition is computed and analyzed and a Lyapunov exponent for the system is defined. The relevance of these networks to biology, their relationships with standard cellular automata and possible extensions are outlined.

PACS number(s): 87.10.+e, 0.5.50.+q, 64.60.Cn

I. INTRODUCTION

One of the most fascinating phenomena displayed by biological systems is the process of morphogenesis. By this process a simple cell replicates and the progeny cells become different from one another via the so-called cellular differentiation. In spite of the well known fact that all cells share the same set of genes, cell division together with further cell-to-cell instructions are able to break the initial symmetry eventually leading to tissues and organs [1]. The great development of molecular biology allows to understand the process of cell differentiation in terms of dynamical rules of gene-gene interaction. But a detailed global picture of the whole process is far away from simple. As with many other complex systems, a large number of units (the genes) influence each other through a complex web of nonlinear interactions. However, some strong regularities allow to describe some relevant features of these systems in statistical terms.

Gene networks have some properties that allow them to be analysed in a systematic way in statistical terms. On one hand, we know that the response of genes to stimulation/inhibition by other genes is typically highly nonlinear but shows saturation in their response [1,2]. This is not different from what is typically assumed in standard neural network models.

Two main statistical approaches to complex regulatory networks have involved discrete dynamical systems and graph-theoretic arguments [2]. In both cases, the units are extremely simple (either binary variables or the nodes of a graph) as well as their “interaction” (simple Boolean functions or directed connections between nodes, respectively). An obvious question to be asked is how robust are these oversimplified pictures of reality as further complexity is added to them. Besides, there is another area of complex systems, that of cellular automata (CA) models [3] where some generic properties have also been identified. In both cases, it has been suggested that the presence of critical points (due to their maximum in-

formation transfer properties, long correlations and high homeostatic stability of attractors) might be particularly relevant to complex systems. However, CA models typically involve a number of possible states larger than two, and thus the properties of these non-binary CA models cannot be easily compared to those displayed by Boolean nets.

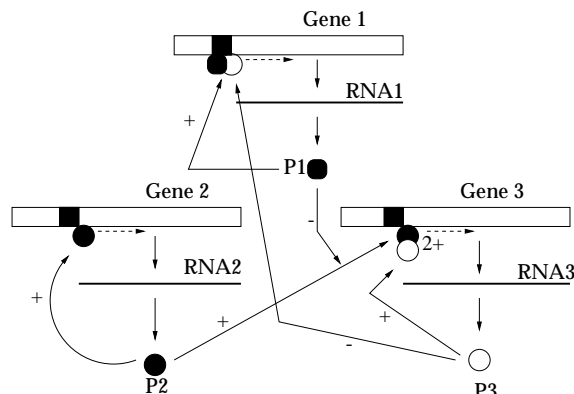


FIG. 1. Gene network with $N = 3$. Here the proteins ($P1, P2, P3$) obtained from each gene interact in complex ways with DNA. The gene products bind some specific sites either in the DNA sequence or on another protein site, thus inhibiting or stimulating gene activity. Several genes can be involved in the regulation of a given gene (as described in RBN models through the connectivity K). But such regulation can have different effects on different genes and under different initial conditions. Here genes 2 and 3 act synergistically stimulating gene 3 in such a way that the latter produces at a rate twice the one expected if gene 2 were repressed by gene 1. If gene 1 starts producing an enough large concentration of $P1$, then it would be able to suppress the stimulation from gene 2 to 3 and thus gene 3 would produce a basal level of protein. If we identify such differences of gene activity levels as gene *states* then we can map the previous example into a discrete model with a number of (multiple) states

At a coarse-grained scale, many complex systems (in-

cluding the genome) can be fairly well understood in terms of a set of such interacting simple units. Sometimes, when these systems are close to critical points, universal properties are at work and a quantitative agreement is obtained. In this context random Boolean networks (RBN) [2] and cellular automata [3] are two key approaches in our understanding of complexity [4]. In both cases, discrete-time and discrete-space are used, together with a finite number of states. For CA, we have a dynamical evolution defined (for the one-dimensional case with a $(2r + 1)$ -neighborhood) by means of:

$$\sigma_i(t + 1) = \Lambda \left[\sigma_{i-r}(t), \sigma_{i-r+1}(t), \dots, \sigma_{i+r}(t) \right] \quad (1)$$

where $i = 1, \dots, N$ and $\sigma_i(t) \in \Sigma \equiv \{0, 1, \dots, S - 1\}$. Here

The function Φ is a given (previously defined) rule [2]. Identical rules are defined for each $(2r + 1)$ -neighborhood. In contrast with this homogeneity in neighbors and rules, RBN's are a particularly interesting class of dynamical systems which shares some properties with CA models, but where randomness is introduced at several levels. Now the dynamics is given by:

$$\sigma_i(t + 1) = \Lambda_i \left[\sigma_{i_1}(t), \sigma_{i_2}(t), \dots, \sigma_{i_K}(t) \right] \quad (2)$$

where $i = 1, \dots, N$ and $\sigma_i(t) \in \Sigma \equiv \{0, 1\}$.

In these models each automaton is randomly connected with exactly K others which send inputs to it. Here Λ_i is a Boolean function also randomly chosen from a set \mathcal{F}_K of all possible K -inputs Boolean functions. In spite of the random selection both of neighbors and Boolean functions, it is well known that a critical connectivity K_c exists where "spontaneous order crystallizes" [3]. In K_c a small number of attractors ($\approx O(\sqrt{N})$) is observed which show high homeostatic stability (i.e. high stability against minimal perturbations in single elements or Boolean functions), and low reachability among different attractors. These properties are consistent with some observations of the genome organization [3,5]. A considerable effort has been dedicated over the last years to the analysis (both theoretical and computational) of the scaling behavior of the numbers and size of cycles close to the critical boundary [5-7].

Alternative models to this problem are provided by neural network-like approaches [8]. In this case we have a dynamical system given by the set:

$$\sigma_i(t + 1) = \Phi \left[J_{ii} \sigma_i(t) + \sum_{l=1}^{K-1} J_{ij_l(i)} \sigma_{j_l(i)}(t) + \theta_i \right] \quad (3)$$

where $\Phi(x)$ is a sigmoidal function which can be asymptotically approached by a step function, i.e. $\Phi(x) = 0$ if $x \leq 0$ and $\Phi(x) = 1$ otherwise. Not surprisingly, neural networks with random connectivities show some of the properties displayed by RBN. Two well-defined phases are also described, which also depend on the input connectivity [9].

Though the picture of on-off genes is a simplified one, in some cases it can be justified from general arguments based on mutual inhibition among genes [10]. Let us consider two given genes which interact among them by means of two given proteins, whose concentrations are indicated by the pair (x, y) . This can be used as a toy model of some well known properties of the life cycle of viruses (like the λ -Phage [3,10]). A theoretical model of mutual inhibition is given by the following couple of cross-inhibitory equations:

$$\frac{dx}{dt} = \frac{\mu^n}{\mu^n + y^n} - x \quad (4.a)$$

$$\frac{dy}{dt} = \frac{\mu^n}{\mu^n + x^n} - y \quad (4.b)$$

where $x, y \in \mathbf{R}^+$. Here $n \in \mathbf{N}$ is a measure of the strength of the interaction. For $\mu = 1/2$, the stability of the fixed point $P^* = (1/2, 1/2)$ is given by the eigenvalues of the Jacobi matrix:

$$L_\mu(P^*) = \begin{pmatrix} -1 & -\frac{n}{2} \\ -\frac{n}{2} & -1 \end{pmatrix} \quad (5)$$

which leads to stability for $n < 2$ and to instability otherwise. For $n > n_c = 2$, P^* becomes a saddle point and two new stable attractors $\{P_+, P_-\}$ are formed (stable nodes). For strong interactions, one of the concentrations dominate over the other and, basically, the two new attractors are simply $P_+ \approx (1, 0)$ and $P_- \approx (0, 1)$. So the result of this interaction between continuous quantities leads to a basically binary outcome [11].

But gene activity can lead to more complex combinations (see figure (1) as example). And in fact experimental analysis of RNA levels in developing embryos shows a wide range of gene activity levels. Different genes interact in very complex ways, and activation or repression takes place in such a way that the same gene can be more or less active depending on the coupling of proteins to different regulatory sites [12]. If we consider a general network formed by m elements showing mutual inhibition, i.e.:

$$\frac{dx_i}{dt} = f_\mu^{(i)}(x_1, x_2, \dots, x_n) = \frac{\mu^n}{\mu^n + \sum_{j \neq i} x_j^n} - x_i \quad (6)$$

With $i = 1, \dots, m$. This network leads to the emergence of a (usually large) number of attractors when n is large enough. In general, for a more complex network, many possible states can be observed, displaying a range of intermediate states. In order to avoid this problem other approximations have been proposed. These approximations retain the discreteness of the units but consider a continuous range of values [11, 14] more close to the real picture, where gene activity can be measured in terms of RNA concentrations [12].

These results makes necessary a generalization of RBNs extending them into a more general framework.

In particular, we can ask how are the critical boundaries defined for a more general situation when multiple states are available. Although the starting point of our study deals with genomic regulatory circuits, a set of different, but related problems could be explored within this framework. If a given state is identified in terms of a cell type, for example, the interactions between different cells (automata) with different cell type will eventually lead to transitions which are known to be rather complex and neighbor-dependent [12]. Another example could be a system where each unit can have a complex internal state roughly characterized by scalar quantity (or "state") which can be, for example, the mean activity. A further scenario where our description applies is a system of machines (computers or agents) each one engaged in a given task. These machines might be connected in complex ways, and switch from a task to another by depending on their actual inputs.

Discrete dynamical systems involving a given range of states per unit are well known in the physics literature. Cellular automata (as described by equation (1)) are just the best known example [2]. Another example from statistical mechanics is the q -Potts model [13] which generalizes the classical Ising spin systems. It well known that this model shows phase transitions with a critical temperature $T_c(q)$ depending on q , the number of possible spin states. Our goal in this paper is to explore the properties of the critical points for S -state random networks. In this context, the analysis of transition phenomena in CA shows that, for large r -neighborhoods, a sharp (second order) transition occurs for well-defined λ -values. However this result cannot be translated to the genome because typically gene regulation is a non-local phenomenon [8,12]. We should expect, however, to find some agreement between the CA results and those derived from networks involving multiple states and random connectivity.

The paper is organized the follows manner: in section II, random networks with multiple states are define and the critical surface in the (K, S, p) space is derived from Derrida's annealed approximation. In the the Appendix I associated with this section a maximum entropy variational approach is used in order to compute the expected distribution of states at criticality. In section III the relationship with CA models for large number of states S is analyzed. In section IV a variant of Flyvbjerg's method of stable core computation is introduced in order to obtain an order parameter (the *self-overlap*) for the transition. In the Appendix II associated with this section we compute a Lyapunov exponent for the system. Finally, a discussion of the general results and possible extensions is given in section V.

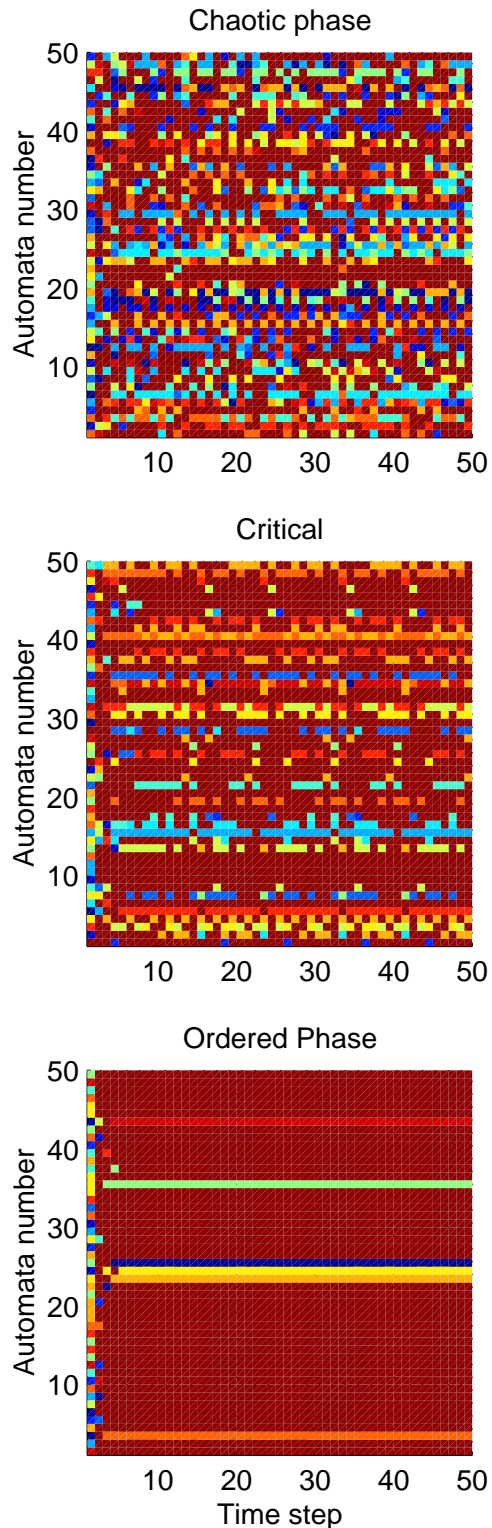


FIG. 2. Space-time diagram for three characteristic cases of RNS with $N = 100, S = 15$ and $K = 2$. Top to bottom: chaotic case with bias $p = 0.55$, critical case with bias $p = 0.70$ and ordered case with bias $p = 0.85$. Here the scale is related with the state of the individual units. Darker squares correspond to higher values of $\sigma_i(t)$

II. THE MODEL AND DERRIDA'S ANNEALED APPROACH

The previous definition of random Boolean network, where $\Sigma = \{0, 1\}$ can be generalized to a wider set of states, $\Sigma = \{0, 1, \dots, S-1\}$ that is to say, to random networks with multiple states (RNS). As with RBN, each element σ_i ($i = 1, \dots, N$) receives K inputs; so we have:

$$\sigma_i(t+1) = \Lambda_i^s \left[\sigma_{i_1}(t), \sigma_{i_2}(t), \dots, \sigma_{i_K}(t) \right] \quad (7)$$

where the superindex s of the functions Λ_i^s indicate that its inputs (and outputs) can take S values and the functions Λ_i^s are randomly chosen from a set $\mathcal{S}_{\mathcal{K}}$.

As with RBNs, this model exhibits three characteristic dynamical regimes, which we will explore. Three examples are shown in figure (2) for a $N = 100$ network with $S = 15$ states, $K = 2$ and different p -values. Here p is an additional which was introduced by B. Derrida et al. [15] in order to make the RBN transition smooth and continuous. The parameter p , known as the bias of Λ_i , is defined as the probability of having 0 as output in the function Λ_i . This parameter is easy to extend in natural form for the RNS (see below). The plots correspond (top to bottom) to the chaotic ($p = 0.55$), critical ($p = 0.70$) and frozen ($p = 0.85$) regimes.

Now in order to characterize the critical properties of our system, we will apply the well known Derrida's method, based on the annealed approximation [15]. This approach is a way to avoid the dynamical correlations which appear as the system evolves in time. In the thermodynamic limit the original (quenched) model and the annealed counterpart share the same phase transition curves [16].

We start with two randomly chosen configurations

$$C_1(t) \equiv (\sigma_1^{(1)}(t), \dots, \sigma_N^{(1)}(t)) \quad (8.a)$$

$$C_2(t) \equiv (\sigma_1^{(2)}(t), \dots, \sigma_N^{(2)}(t)) \quad (8.b)$$

which are also randomly taken from the set $\mathcal{C}_S(N)$ of all the possible N -strings (clearly $\#\mathcal{C}_S(N) = S^N$). Following Derrida's method, it can be shown that the overlap $a_{12}(t) \in [0, 1]$, defined as the normalized number $Na_{12}(t)$ of elements with common states in $C_1(t)$ and $C_2(t)$, will evolve in time following a nonlinear one-dimensional map. In short, let $Na_{12}(t+1)$ the net overlap after one iteration of $C_1(t)$ and $C_2(t)$ under (7). Then a new set of connections and Λ_i^s functions is again taken from $\mathcal{S}_{\mathcal{K}}$, and a new iteration is performed over $C_1(t+1)$ and $C_2(t+1)$.

For our S -state random network and assuming that $\frac{1}{S}$ is the probability that two outputs of an arbitrary function Λ_i^s are identical, following the arguments in [15], we have a nonlinear map for a_{12} given by:

$$a_{12}(t+1) = a_{12}^K(t) + \frac{1}{S} \left[1 - a_{12}^K(t) \right] \quad (9)$$

where: $a_{12}^K(t)$ is the fraction of elements with identical inputs and $[1 - a_{12}^K(t)]/S$ is the probability for two automata, with at least one different input, being equal at $t+1$. Now the critical point where the phase transition takes place (separating the so called frozen and chaotic phases) is obtained from the stability condition:

$$\left. \frac{\partial a_{12}(t+1)}{\partial a_{12}(t)} \right|_{a^*=1} = K \left(1 - \frac{1}{S} \right) \leq 1 \quad (10)$$

or in other words the following relation between the average network connectivity and the number of available states is reached:

$$K = \frac{1}{1 - \frac{1}{S}} \quad (11)$$

We see that for $S = 2$ (Boolean net) we recover the well known critical point $K_c = 2$. For $S \gg 2$ we can approximate the marginal stability relation to:

$$K \approx 1 + \frac{1}{S} \quad (12)$$

We also see that when $S \rightarrow \infty$ the average connectivity moves to $K_c \rightarrow 1$ (i.e. the critical point is reached only at the lowest connectivity). The previous inequality (10) is related with the high-temperature value of damage spreading [23] of the Potts model [13].

In RNS it is possible to extend Derrida's p -parameter definition: p is defined as the probability of having a 0 as output of the function Λ_i^s (0 is the quiescent state) and the other states are equally likely to be present. Although this choice seems too limited, it can be justified from variational arguments (see Appendix I). Now the overlap will evolve following the 1D map:

$$a_{12}(t+1) = a_{12}^K(t) + \left[p^2 + \frac{(1-p)^2}{S-1} \right] (1 - a_{12}^K(t)) \quad (13)$$

where we have:

- $a_{12}^K(t)$ is the fraction of elements with identical inputs at time t
- $(1 - a_{12}^K(t))p^2$ is the probability of two automata with at least one different input, being equal to "0" at $t+1$.
- $(1 - a_{12}^K(t))(1-p)^2/(S-1)$ gives the probability of finding two automata with at least one different input, being equal (but different from 0) at $t+1$.

Now, the stability analysis for $a_{12}^* = 1$ gives us a general condition for the critical points:

$$p_c = \frac{1}{S} \left[1 + \left(1 - \frac{S}{K} \left[(2-S)K + S - 1 \right] \right)^{1/2} \right] \quad (14)$$

Defining a critical surface $p_c = p_c(K, S)$ separating the frozen (ordered) phase from the chaotic one.

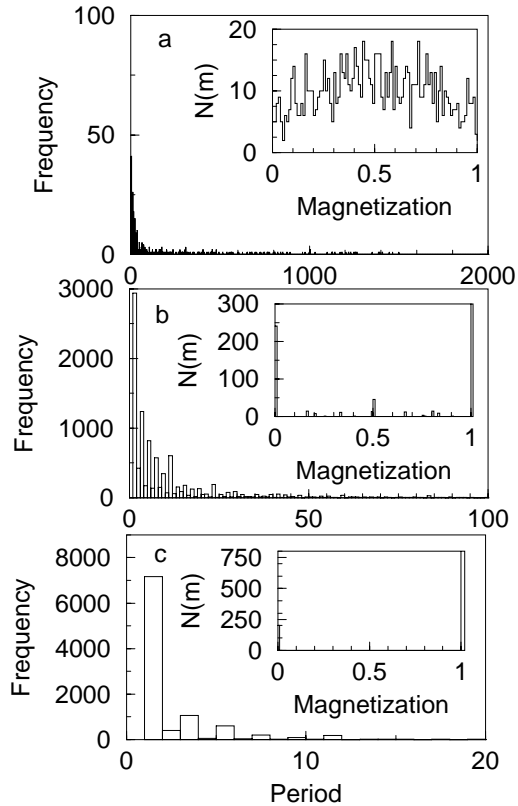


FIG. 3. Distributions of cycle lengths for the three different regimes of a RNS with $K = 2, S = 5$ (here 10^4 different RNS have been used, with random connectivities and random initial conditions). Here: (a) $p = 0.60$, chaos, (b) $p = 0.689$, critical and (c) $p = 0.8$, frozen regime, respectively. Insets: Distribution of magnetization m for the three different regimes. These distributions have been calculated using a $N = 100$ network and averaging over $\tau = 10^4$ steps after 10^4 transients have been removed.

A numerical characterization of these three regimes can be easily obtained by computing the frequency distribution $N(T)$ of cycles of different length T . Since these dynamical systems are finite, with a maximum number of S^N states, the previous equations (7) lead to two types of attractors (cycles and steady states). However, the presence of a critical boundary separating the two regimes is made clear by the existence of well-defined scaling laws. In figure (3.a-c) we show the frequency distribution of periods (cycle lengths) for the three regimes. At the chaotic phase (figure (3.a)), long-periodic orbits are rather common. This is due to the exponential increase of attractor lengths in this phase. The frozen regime (figure (3.c)) shows the opposite tendency: the periods are very short, with an exponential decay with T . At the critical boundary (figure (3.b)), both short and long periods are present, in such a way that in spite of the frequent

observation of short-period orbits, long-periodic orbits of length $T \approx O(N)$ are always found. In the insets of the previous plots we also show three examples of the magnetization m (for different RNS with $N = 100, K = 2$ and $S = 5$ states). Here m is defined as the number of times n a given automaton S_i is such that $S_i = 0$ over T steps i. e. $m = n/T$. Then $P(m)$ is a histogram giving the distribution of m for the whole system i. e. it counts the number of automata with the same average magnetization m . We can see, as expected, how $P(m)$ moves from a singular distribution with few peaks at the frozen regime to a more continuous distribution at the chaotic regime.

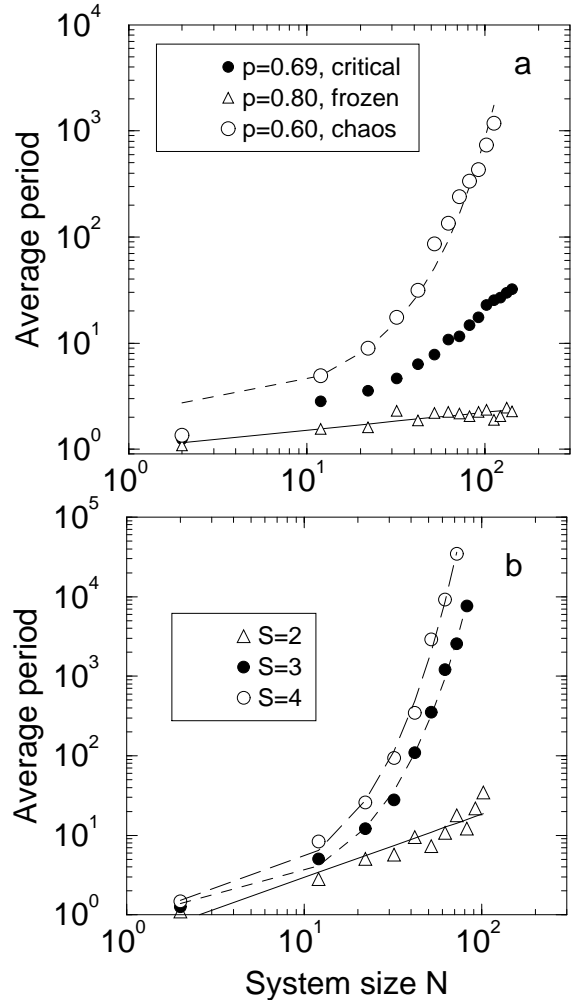


FIG. 4. Average period length versus system size for RNS with (a) $S = 5, K = 2$ and different biases and for (b) $p = 0.5, K = 2$ and different numbers of states

In random Boolean networks, the previous observations have been deeply explored through both numerical and theoretical approximations [6,7]. A specially important relation is the dependence of the average period $\langle T \rangle$ with the system size N . When RBN are used with

$p = 0.5$, it is found that the critical phase ($K = 2$) is characterized by a scaling $\langle T \rangle \approx \sqrt{N}$ and an exponential growth $\langle T(K > 2) \rangle \approx 2^{BN}$ is obtained at the chaotic phase, with $B > 1$ [2]. We have explored this scaling behavior in the RNS counterpart. Two examples of our calculations are shown in figure 4(a-b). The average period length has been calculated in two different cases, by (a) varying p and (b) the number of states S . We can see how the scaling $\langle T(N) \rangle \approx N^\tau$ is present at criticality and how an exponential increase in $\langle T \rangle$ also appears as we enter into the chaotic phase. Numerical simulations show that for the chaotic phase an exponential law $\langle T(S, N) \rangle \approx S^{BN}$ is obtained, with $B > 1$. Numerical estimations of this value gave $B = 1.11 \pm 0.02$.

III. CA AND RNS

It can easily be checked from (14) that for $S = 2$ (Boolean net) we have

$$p_c = \frac{1}{2} + \frac{1}{2} \sqrt{1 - \frac{2}{K}} \quad (15)$$

which gives us the well known critical line in the (K, p) -phase space [15,17].

Equation (15) is reminiscent of those found in standard CA (with nearest-neighbor connectivity [18]). The existence of a transition domain for CA models has been characterized by means of several approaches. Langton's λ -parameter gives a rough characterization of these critical points when complex CA rules (involving high S and/or r values) are used. If S^{2r+1} is the total number of $(2r+1)$ -configurations in the CA rule table, as described by (1), and M out of the total map to a non-zero state, then λ is defined as [18]:

$$\lambda \equiv \frac{M}{S^{2r+1}} \quad (16)$$

Thus, $1 - \lambda$ corresponds to p under the RNS definition. This parameter has been shown to be related with -but not equivalent to- a temperature in statistical physics [18]. It was observed (particularly in the large- r limit) that these CA exhibit some of the characteristics of second-order phase transitions (for a detailed study see [18], strictly speaking although the association between computation, complexity and critical phenomena has been shown to be flawed [19]). Li et al. [18] showed by means of mean field approximations that, for $S = 2$, there is a simple relationship between the critical value λ_c and r (the neighborhood radius):

$$1 - \lambda_c = \frac{1}{2} + \frac{1}{2} \sqrt{1 - \frac{2}{r+1}} \quad (17)$$

This result is consistent with equation (15). But in (17), instead of $2r+1$ (the total connectivity of the CA model)

we have $r+1$ (half of it plus one). In the RNS counterpart, we have K , the total connectivity. These differences are due to the spatial correlations intrinsic to CA models, which are destroyed in the RNS counterpart. This is consistent with the analysis of Li et al. [18] which is based in a mean-field estimation of the spreading rate of different CA patterns. Assuming symmetry in the average spreading rate $\gamma(r)$ in right and left directions, they obtain the onset to non-zero spreading at λ_c given by (17). The corresponding critical curves for both the $1 - \lambda$ parameter (squares) and p (circles) as a function of the connectivity are shown in figure (5). Remember that a neighbor radius r in CA is equivalent to $K = 2r + 1$ in RNS. Thus the first point represented for RNS with $S = 2$ is $K = 3$ with $p_c = 0.79$. Both curves share the same qualitative behavior, but larger values of the bias are required in RNS in relation with CA in order to reach the ordered regime, as expected. A similar relationship is found for the temperature in relation with q in some q -Potts models [13].

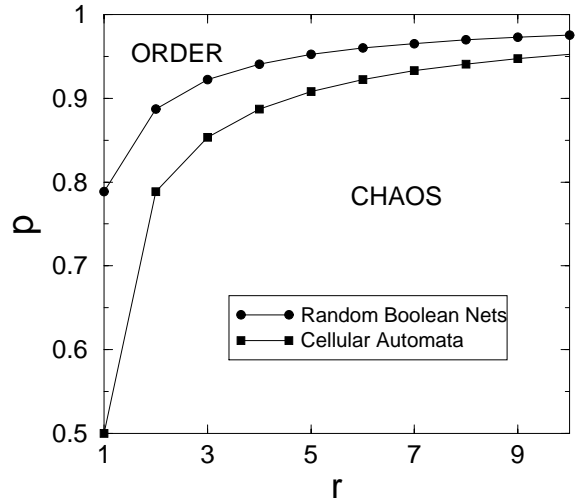


FIG. 5. Phase diagram obtained from mean field theories for both RNS and CA models (with $S = 2$). Here the fraction of transitions towards the quiescent state 0 is plotted against neighbor radius. This fraction is named p for RBN (filled circles) and $1 - \lambda$ for CA (filled squares). The equivalent neighbor radius for RBN is $K = 2r + 1$.

IV. STABLE CORE AND THE SELF-OVERLAP METHOD

A well-defined critical phase transition should be characterized by an appropriate order parameter Ω such that $\Omega > 0$ at the disordered regime and zero otherwise. In fact, $d^* = 1 - a^*$ order parameter for RBN and RNS [15]. In this context, Flyvbjerg [22] explored a different approach than Derrida's by defining the *stable core* at time t , $c(t)$, as the (normalized) fraction of automata S_i (independent of the initial condition) that reach stable values at a given step t , i.e. remain constant after t . The

stable core asymptotic behavior, $c(t \rightarrow \infty)$, can be used as an order parameter for the frozen-chaos transition in RBN. Explicitly, if $\Omega \equiv 1 - c(t \rightarrow \infty)$, the previous requirements for the order parameter definition hold.

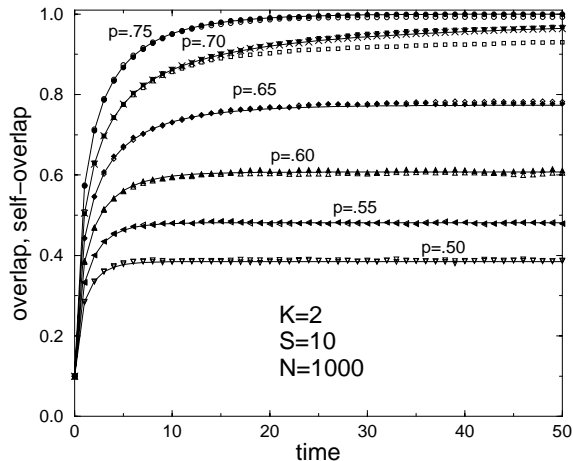


FIG. 6. Continuous lines: dynamical evolution of the self-overlap for $K = 2$, $S = 10$ and varying p , with initial self-overlap (and overlap) of 0.1 (see text). The black symbols are numerical averages of the overlap between two RNS for 100 quenched replicas experiments with $N = 1000$. The white symbols are results for self-overlap with identical averages and conditions, except for the white squares where $N = 10000$ for critical $p = 0.70$ in order to show the finite size effect of the critical transition

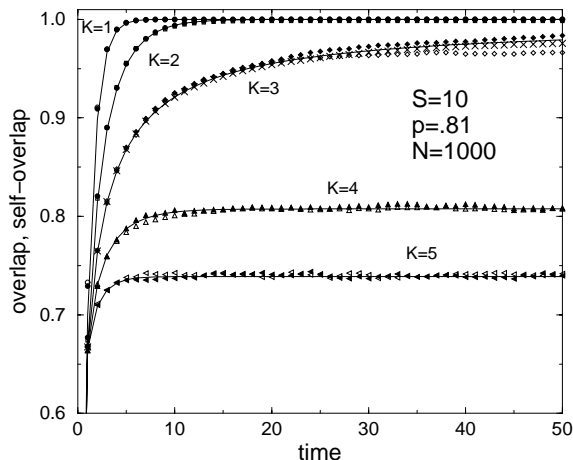


FIG. 7. Same as in figure 8, now with $p = 0.81$, $S = 10$ and varying K .

The argument of Flyvbjerg for finding an iterated equation for $c(t)$ is as follows. There are $K + 1$ mutually exclusive reasons for a given automata S_i to be part of the stable core from step t to $t + 1$. The probabilities of this $K + 1$ reasons are: (0) All the inputs, $\sigma_{i_1}(t), \sigma_{i_2}(t), \dots, \sigma_{i_K}(t)$, belong to the stable core at t . Given that the inputs are chosen at random, this situation occur with probability $c^K(t)$ (where $c(t)$ is inter-

preted as the probability of belonging to the stable core in t).

(1) Λ_i is independent of one input and the rest of the $K - 1$ variables belong to the stable core:

$$\binom{K}{1} c^{K-1}(t)(1 - c(t))p_1 \quad (18)$$

where p_1 is defined as the probability of Λ_i to be independent of one input after fixing its $K - 1$ remainder inputs.

⋮

(j) Λ_i is independent of j inputs and the rest of the $K - j$ variables belong to the stable core:

$$\binom{K}{j} c^{K-j}(t)(1 - c(t))^j p_j \quad (19)$$

where p_j is defined as the probability of Λ_i to be independent of j arguments after fixing its $K - j$ remainder arguments.

⋮

(K) Λ_i^s is a constant function (independent of its K arguments), with all out the stable core:

$$(1 - c(t))^K p_K \quad (20)$$

Adding the $K + 1$ exclusive reasons:

$$s(t + 1) = \sum_{i=0}^K \binom{K}{i} c^{K-i}(t)(1 - c(t))^i p_i \quad (21)$$

where p_i is the probability that the Boolean function is independent of a certain number i of inputs after fixing its $K - i$ remainder inputs (a biologically relevant case are the canalizing functions that depend on a unique input and are independent of remainder [2]). For the Boolean functions with bias p , i.e., with value 0 with probability p and value 1 with probability $(1 - p)$ it gives:

$$p_i = p^{2^i} + (1 - p)^{2^i} \quad (22)$$

By substituting (22) into (21) and analyzing its stability the following transition critical curve is obtained: $K2p(1 - p) = 1$ according to [15,23], reached by different methods.

How to extend this argument to RNS? Apparently, such an extension is straightforward. It seems that, again, there are $K + 1$ exclusive reasons for a given automata to move from outside the stable core to be a member of it. However, a simple translation of the previous procedure is not possible, and we can show why by means of a simple example. Let us consider a RNS with $K = 4$ and $S = 3$, i.e.:

$$\Lambda_i^3 = \Lambda_i(\sigma_{i_1}, \sigma_{i_2}, \sigma_{i_3}, \sigma_{i_4}) \quad ; \quad i = 1, 2, \dots, N \quad (23)$$

and let us assume that at a given t the first three inputs belong to the stable core, i.e: $\sigma_{i_1}, \sigma_{i_2}, \sigma_{i_3} \in s(t)$ and

$\sigma_{i_4} \notin s(t)$. The question is whether or not $\sigma_i(t+1) \in s(t+1)$ if $\sigma_i(t) \notin s(t)$. This will happen if Λ_i^3 is independent of the fourth input. But it can also occur (and this makes a big difference) if σ_{i_4} can only reach a subset $\Sigma' \subset \Sigma$, say $\Sigma' \equiv \{0, 1\}$. In such case, we have a reduction in the number of degrees of freedom for σ_{i_4} . In this case it can happen that Λ_i^3 is independent of σ_{i_4} for $\sigma_{i_4} \in \Sigma'$ but not if $\sigma_{i_4} = 2$ (for $S = 2$ a reduction of one degree of freedom simply means that the input belongs to the stable core). These possible outcomes forces us to weight the probabilities that the input units have their degrees of freedom reduced. More generally, the exclusive reason (1) implies that Λ_i^3 is independent of a given input σ_{i_j} . This occurs with probability $p_1 = p^2 + (1-p)^2$ for the case of two states. For S states, it can occur that $\sigma_{i_j} \in \Sigma' \subset \Sigma$ and $\sigma_{i_j} \notin s(t)$. In order to calculate the order parameter equation for networks with multiple states, we will compute the successive overlap (or *self-overlap* [25]) $a(t)$, defined as the fraction of automata such that: $\sigma_i(t) = \sigma_i(t-1)$. This is in fact the overlap between the system configuration at t with the next configuration at $t-1$. If the asymptotic value of the stable core is 1 the self-overlap $a(t \rightarrow \infty)$ will be one too. This allows us to use the asymptotic value of the self-overlap as an appropriate order parameter and as an alternative to the standard overlap equation analyzed in section II.

The iterated map for the self-overlap will be

$$a(t+1) = a(t)^K + \left(p^2 + \frac{(1-p)^2}{S-1} \right) (1 - a(t)^K) \quad (24)$$

where we describe the self-overlap between the set at $t+1$ and t as a function of the self-overlap for $(t-1, t)$. If we interpret $a(t)$ as the probability for an arbitrary unit to remain in the same state at both $t-1$ and t , the term $a(t)^K$ gives the probability that all the inputs of a given unit are the same from $t-1$ to t . Obviously $(1 - a(t)^K)$ is the probability that at least one of the inputs will be different between t and $t-1$. In that case, there is still the possibility of remaining in the same state at t and at $t+1$ just by chance. This is given by $(p^2 + (1-p)^2)/(S-1)$.

The stability analysis now gives:

$$\left. \frac{\partial a(t+1)}{\partial a(t)} \right|_{a^*} = K \left[1 - \left(p^2 + \frac{(1-p)^2}{S-1} \right) \right] \leq 1 \quad (25)$$

which is easily interpreted from a perturbative point of view [23]: $p^2 + \frac{(1-p)^2}{S-1}$ is the probability of no-propagation for the minimal perturbation (one change of state l to m in one input). Then, $K \left[1 - \left(p^2 + \frac{(1-p)^2}{S-1} \right) \right]$ is the mean number of changes generated by the perturbation in one time step. This interpretation allows to define a Lyapunov exponent for this system (see Appendix II).

In figures (6-7) we show (continuous lines) the asymptotic behavior of both the overlap and the self-overlap for different p and K (for $S = 10$) from equation (24). As we can see, the dynamical equation for the self-overlap

(24) is the same as the standard overlap equation (13), although it is conceptually different from it. The self-overlap, as it occurs with the stable core, can only be applied to the quenched system but not to the annealed case. Besides, the self-overlap is computationally more efficient than the standard overlap, which requires the parallel running of the two replicas of the system.

In figure (6) we have followed the time evolution (black symbols) of overlaps between two RNS quenched replicas of size $N = 1000$ as in [15]. Each point is computed by averaging over 100 experiments and different p values are used. The connectivity ($K = 2$) and the number of available states ($S = 10$) are fixed. The white symbols represent identical averages for self-overlap, except for the white squares where $N = 10000$ for critical $p = 0.70$ in order to show the finite size effect of the critical transition. This effect is more accused for the self-overlap as for the overlap.

In figure (7) we show the time evolution with $S = 10$, $p = 0.81$ and varying K , for both the overlap and the self-overlap. Again the continuous lines are the theoretical evolution from equation (29). Black and white symbols correspond to overlap and self-overlap respectively. In this case the variation of the connectivity despite the transition at $K_c = 3$. The white diamonds ($N = 10.000$ for self-overlap) show the finite size effect.

All our simulations show a very good agreement with the theoretical evolution of the overlap (13) and the self-overlap (24). In this sense, both can be used as appropriate order parameters.

V. SUMMARY

In this paper we have proposed a simple, straightforward extension of random Boolean networks in terms of a discrete model with multiple states. The starting point of our analysis is the observation that several natural systems involving a wired set of entities of some kind often display a range of state values instead of simple on-off characteristics. In some cases, as the specific tasks (states) performed by ants in a colony, the discreteness of the states is rather well defined, although their transitions (as a consequence of interactions of ants engaged in different tasks) can be rather complex [24] suggesting that the underlying task-dependent rules are complicated ones. When cell types are considered, we also get a well-defined set of "states" although each one itself is the result of a complex dynamical system (the gene expression pattern) at a given stationary state. In this context, a classical set of experiments with different organisms at different levels of development reported the existence of complex interactions between cell types eventually leading to switches by depending of the cell types under interaction [2,12]. In other systems, such as gene regulatory networks, the activity of some genes is sometimes close to an on-off switch but it displays a range of

activity levels. A first approximation to such continuous networks is the RNS described and analyzed in this paper. Following previous studies, our interest was focused on the critical features of these networks. It has been conjectured that a wide range of complex systems, from evolving ecosystems, biological regulation networks, traffic or ant colonies [4], to cite only a few, display patterns in space and time suggesting that they are close to phase transition points. In this context, we have found the explicit form of the transition domains as well as an order parameter equation for the transition.

The critical boundaries for this model have been obtained from Derrida's annealed approximation and the computation of $s(t)$ (the stable core equation) required the development of an alternative treatment to the Flyvbjerg derivations for standard RBN [22]. This model has been shown to share some common traits with other related dynamic models like cellular automata and the q -Potts model.

Several extensions of this work are possible. Further quantities can be defined in order to characterize the damage spreading. This can be easily done by means of theoretical extensions of previous definitions of Lyapunov exponents for RBNs [25]. One of them is the analysis of the square-lattice counterpart of the RNS with nearest-neighbor connectivity. This type of network has been proved to be extremely useful in order to display the critical features of the RBN model in terms of percolation on a square lattice [15]. A different extension would be a re-definition of the network rules in order to make the transitions from different states closer to the continuous dynamics. If the output of the Λ_i^s function is randomly chosen from Σ , we must expect to observe a time evolution of individual units in terms of jumps from a given state to any other state. But if we want to retain the relationship between the S -state model with the corresponding continuous counterpart (as described by sets of nonlinear differential equations) a consistent increase or decrease in individual activity should be observable. This problem can be easily solved through the introduction of a new set of rules describing the outputs of the Λ_i^s -function in terms of increases/decreases of gene activity and will be reported elsewhere.

Acknowledgments:The authors would like to thank Andy Wuensche, Brian Goodwin, Isaac Salazar-Ciudad, Jordi Delgado and Mar Cabeza for useful discussions. This work has been partially supported by a grant DGYCIT PB-97-0693 and by the Santa Fe Institute (RVS and SK) and by the Centro de Astrobiología (BL).

VI. APPENDIX I: RNS AND MAXIMUM ENTROPY

The relation (11) can be easily generalized: K can be not unique, but an average connectivity $\langle K \rangle$ is always

able to be defined [17] and we can have a probability distribution of states, i.e. $P(\mu) = P[\Lambda_i^S = \mu]$ for $\mu \in \Sigma$. In this general case, the critical line transition is given by: $\langle K \rangle = 1/(1 - \sum P^2(\mu))$ [23]. This result can be used in order to find the expected probability distribution of states at criticality [17]. Using the following maximum entropy constraints:

$$\sum_{\mu} P(\mu) = 1 \quad (1)$$

$$\sum_{\mu} P^2(\mu) = 1 - \frac{1}{\langle K \rangle} \quad (2)$$

$P_c^*(\mu)$ can be derived from a variational procedure known as the maximum entropy formalism [20]. We first construct the Lagrangian:

$$\begin{aligned} \mathcal{L}(\mathbf{P}) = & - \sum_{\mu} P(\mu) \log P(\mu) - \\ & - \beta \left(\sum_{\mu} P^2(\mu) - \frac{1}{\langle K \rangle} \right) - \\ & - \alpha \left(\sum_{\mu} P(\mu) - 1 \right) \end{aligned} \quad (3)$$

where $\mathbf{P} = (P(0), P(1), \dots, P(S-1))$ and the variation

$$\frac{\partial \mathcal{L}(\mathbf{P})}{\partial \mathbf{P}} = 0 \quad (4)$$

is performed. This leads to a set of equations

$$\log P(\mu) + 2P(\mu)\beta = -(1 + \alpha) \quad (5)$$

which must be solved for $P(\mu)$. Let us introduce $P(0) = w$ and $P(\mu \neq 0) = \alpha_{\mu}w$ with $\mu = 1, 2, \dots, S-1$ with $w \in [0, 1]$ and $\{\alpha_{\mu}\}$ is a set of positive constants such that

$$w \left(1 + \sum_{\mu=1}^{S-1} \alpha_{\mu} \right) = 1 \quad (6)$$

Then we get:

$$\log w + 2\beta w = -(1 + \alpha)$$

$$\log w + \log \alpha_{\mu} + 2\beta \alpha_{\mu} w = -(1 + \alpha) \quad \mu = 1, 2, \dots, S-1 \quad (7)$$

So $\alpha_{\mu} = C$ (constant) $\forall \mu$ and as a consequence

$$P(0) = w \quad (8.a)$$

$$P(\mu) = \frac{1-w}{S-1} \quad \mu = 1, 2, \dots, S-1 \quad (8.b)$$

The most likely probability distribution close to criticality will be a delta-shaped $P(\mu)$ with a given state present with probability w and the rest equally distributed. We should note that this property (i.e. a sharply peaked distribution with one or a few predominant states) has been reported for the onset of chaos in low-dimensional chaotic dynamical systems [21]. Here the probability distributions maximize a previously defined complexity measure \mathcal{C} and numerical simulations of RNS indeed show that such singular distribution with one or a few peaks is characteristic at criticality.

VII. APPENDIX II: LYAPUNOV EXPONENTS FOR RNS

By following the distance method (or Derrida's approximation) we can interpret the replica of the one system as a perturbation on the original system [25] and we can easily define an expansion rate of the perturbation at time t for RNS:

$$\eta(t) = \frac{d_{12}(t+1)}{d_{12}(t)} \quad (1)$$

Where $d_{12}(t) = 1 - a_{12}(t)$. In a natural way, we can define the Lyapunov exponent as the time average of the logarithm of the expansion rate:

$$\lambda(T) = \frac{1}{T} \sum_{t=1}^T \log \eta(t) = \log \sqrt[T]{\prod_{t=1}^T \eta(t)} = \log \bar{\eta} \quad (2)$$

If we use the equation for the distance between configurations:

$$d_{12}(t+1) = \left(p^2 + \frac{(1-p)^2}{S-1} \right) [1 - (1 - d_{12}(t))^K] \quad (3)$$

Then the expansion rate of the perturbation at time t , is defined by:

$$\eta(t) = \frac{d_{12}(t+1)}{d_{12}(t)} = \frac{\left(p^2 + \frac{(1-p)^2}{S-1} \right) \{1 - [1 - d_{12}(t)]^K\}}{d_{12}(t)} \quad (4)$$

For small $d(t)$, we can write:

$$(1 - d_{12}(t))^K \approx 1 - K d_{12}(t) \quad (5)$$

and thus we have:

$$\eta(t) \approx \left(p^2 + \frac{(1-p)^2}{S-1} \right) K \quad (6)$$

An average constant expansion rate that give us the Lyapunov exponent:

$$\lambda = \log \left[\left(p^2 + \frac{(1-p)^2}{S-1} \right) K \right] \quad (7)$$

that determines the two known regimes: $\lambda < 0$ (order) and $\lambda > 0$ (chaos), with the marginal case $\lambda = 0$, in agreement with the transition surface (14).

There are different methods to compute the largest Lyapunov exponent. Here we will demonstrate that it is possible compute Lyapunov exponents from the self-overlap in agreement with the previous results. The Wolf's method [26] is used to estimate numerically the Lyapunov exponents from time series. In short, the method is described as follows: take two points of the temporal series, say $\mathbf{X}(t_1)$ and $\mathbf{X}(t_2)$ and calculate their distance: $|\mathbf{X}(t_2) - \mathbf{X}(t_1)|$. Assume that $|\mathbf{X}(t_2) - \mathbf{X}(t_1)| < \epsilon$, being $\epsilon > 0$ small. Next, compute the distance, after a time T , i.e. $|\mathbf{X}(t_2+T) - \mathbf{X}(t_1+T)|$. An appropriate T must be chosen [26]. By averaging over n pairs, we obtain an estimation of the Lyapunov exponent:

$$\lambda = \frac{1}{nT} \sum_{t_2 \neq t_1}^n \log \frac{|\mathbf{X}(t_2+T) - \mathbf{X}(t_1+T)|}{|\mathbf{X}(t_2) - \mathbf{X}(t_1)|} \quad (8)$$

For RNS, we can write down an equation for the normalized Hamming distance between successive time steps in our system, i.e. for the complementary probability of the self-overlap: $d(t) = 1 - a(t)$. Thus the equation for the self-overlap becomes:

$$d(t+1) = \left[1 - \left(p^2 + \frac{(1-p)^2}{S-1} \right) \right] [1 - (1 - d(t))^K] \quad (9)$$

If we linearly approximate the previous equation close to the fixed point $d^* = 0$. We get:

$$d(t+1) = K \left[1 - \left(p^2 + \frac{(1-p)^2}{S-1} \right) \right] d(t) \quad (10)$$

The iterated equation now gives:

$$d(t+T) = \left\{ K \left[1 - \left(p^2 + \frac{(1-p)^2}{S-1} \right) \right] \right\}^T d(t) \quad (11)$$

To compute (8) in our terms, and taking $t_2 = t_1 + 1$ (here $T = 1$, the characteristic time step in our system), we have:

$$\frac{d(t+T)}{d(t)} = \left\{ K \left[1 - \left(p^2 + \frac{(1-p)^2}{S-1} \right) \right] \right\}^T \quad (12)$$

a constant value that, once introduced in the sum (8), determines the Lyapunov exponent (7) as suggested previously.

1. L. Wolpert, *Principles of Development* (Oxford U. Press, London, 1998); J. Gerhardt and M. Kirschner, *Cells, Embryos and Evolution* (Blackwell Science, 1997)

2. S. A. Kauffman, J. Theor. Biol. 22 (1969) 437; J. Theor. Biol. 44 (1974) 167; Physica D10 (1984) 145; Physica D42 (1990) 135; S. A. Kauffman, *The Origins of Order* Oxford U. Press (Oxford, 1993); R. Somogyi and C. A. Sniegoski, Complexity 4 (1996) 45; More recently, extensive simulation studies on continuous models of gene networks involving ordinary differential equations have shown that some of the key results of Kauffman studies remain basically the same: see R. V. Solé et al., SFI Working Paper 99-11-075 (1999)
3. S. Wolfram, Physica D10 (1984) 1; A. Wuensche, *The global dynamics of cellular automata*, SFI studies in the sciences of complexity, Addison-Wesley, 1992; Wuensche has done a remarkable research on the basins of attraction of both cellular automata and random Boolean networks; the basic software, named DDLab, is available in the website: <http://www.santafe.edu/wuensche/ddlab.html>.
4. D. Kaplan and L. Glass, *Understanding Nonlinear Dynamics*, Springer-Verlag (New York 1995);
5. R.V. Solé, S.C. Manrubia, B. Luque, J. Delgado and J. Bascompte, Complexity 1(4) (1995) 13
6. R.J. Bagley and L. Glass, J. theor. Biol. 183 (1996) 269
7. U. Bastolla and G. Parisi, Physica D 98 (1996) 1; U. Bastolla and G. Parisi, J. Phys. A: Math. Gen. 30 (1997) 5613
8. A. Battacharijya and S. Liang, Physica D95 (1996) 29; A. Battacharijya and S. Liang, Phys. Rev. Lett. 77 (1996) 1644
9. J. A. de Sales, M.L. Martins and D.A. Stariolo Phys. Rev. E 55 (1997) 3262. In this paper the authors study the overall behavior of gene networks by means of a model involving both short- and long-range couplings among genes. They found a rich variety of behaviors and their results consistently fitted known scaling laws for the number of differentiated cells and cell length cycles as a function of N .
10. K.E. Kurten, Phys. Lett. A 129, 157 (1992)
11. S.L. Adhya and D. F. Ward, Prog. Nucleic Acid Res. Mol. Biol. 26 (1981) 103
12. L. Glass and S.A. Kauffman, J. theor. Biol. 39 (1973) 103; see also L. Glass and S. A. Kauffman, J. Theor. Biol. 34 (1972) 219
13. S. F. Gilbert, *Developmental Biology*, Sinauer, Massachusetts (1996); B.C. Goodwin Temporal organization in cells London, Academic Press (1963)
14. F. Y. Wu, Rev. Mod. Phys. 54 (1982) 235; C. Tsallis and A. C. N. de Magalhaes, Phys. Rep. 268 (1996) 305
15. J. E. Lewis and L. Glass, Int. J. Bif. Chaos 1 (1991) 477; T. Mestl, R. J. Bagley and L. Glass, Phys. Rev. Lett. 79 (1997) 653; A. Wagner, Proc. Natl. Acad. Sci. USA 91 (1994) 4387. These authors consider a simple formulation of biological regulatory networks in terms of a neural-like dynamics, as defined by: $\frac{dx_i}{dt} = -x_i \Phi_i \left(\sum_j W_{ij} x_j - \Theta_i \right)$, with $i, j = 1, 2, \dots, N$. As usual $\Phi(z)$ is a sigmoidal function and θ a threshold. The matrix $W_{ij} \in \mathfrak{R}$ describes the specific features of the interactions among different elements (genes). We can see that equations (4.a-b) are just a specific example with $N = 2$, $\Theta_i = 0$, $W_{ij} = 1$ and $\Theta(z) = \mu^n / (\mu^n + z^n)$.
16. B. Derrida and Y. Pomeau, Europhys. Lett. 1 (1986) 45; B. Derrida and Y. Pomeau, Europhys. Lett. 2 (1986) 739; G. Weisbuch and D. Stauffer, J. Physique 48 (1987) 11-18
17. H.J. Hilhorst and M. Nijmayer, J. Physique 48 (1987) 185
18. R. V. Solé and B. Luque, Phys. Lett. A196 (1995) 331
19. C. G. Langton, Physica D52 (1990) 12; W. Li, N. H. Packard and C. G. Langton, Physica D45 (1990) 77; W. K. Wootters and C. G. Langton, Physica D45 (1990) 95
20. A. Dhar, P. Lakdawala, G. Mandal and S. R. Wadia. Phys. Rev. E51 (1995) 3032
21. H. Haken, Information and self-organization, Springer, Berlin, 1988; J. N. Kapur, Maximum Entropy models in Science and Engineering, Wiley, New Delhi, 1993
22. C. Anteneodo and A. R. Plastino, Phys. Lett. A223 (1996) 348
23. H. Flyvbjerg, J. Phys. A: Math. Gen. 21 L955 (1988)
24. B. Luque and R. V. Solé, Phys. Rev. 55, 1 (1997)
25. R. V. Solé and O. Miramontes, Physica D80 (1995) 171 and references cited
26. B. Luque and R. V. Solé, adap-org/9907001
27. A. Wolf, J. B. Swift, H. L. Swinney and J. A. Vastano, Physica D16 (1985) 285

